LETTER

doi:10.1038/nature11868

Sodium chloride drives autoimmune disease by the induction of pathogenic T_H17 cells

Markus Kleinewietfeld[1,2], Arndt Manzel[3,4], Jens Titze[5,6], Heda Kvakan[7,8], Nir Yosef[2], Ralf A. Linker[3], Dominik N. Muller[7,9]* & David A. Hafler[1,2]*

There has been a marked increase in the incidence of autoimmune diseases in the past half-century. Although the underlying genetic basis of this class of diseases has recently been elucidated, implicating predominantly immune-response genes[1], changes in environmental factors must ultimately be driving this increase. The newly identified population of interleukin (IL)-17-producing $CD4^+$ helper T cells (T_H17 cells) has a pivotal role in autoimmune diseases[2]. Pathogenic IL-23-dependent T_H17 cells have been shown to be critical for the development of experimental autoimmune encephalomyelitis (EAE), an animal model for multiple sclerosis, and genetic risk factors associated with multiple sclerosis are related to the IL-23–T_H17 pathway[1,2]. However, little is known about the environmental factors that directly influence T_H17 cells. Here we show that increased salt (sodium chloride, NaCl) concentrations found locally under physiological conditions *in vivo* markedly boost the induction of murine and human T_H17 cells. High-salt conditions activate the p38/MAPK pathway involving nuclear factor of activated T cells 5 (NFAT5; also called TONEBP) and serum/glucocorticoid-regulated kinase 1 (SGK1) during cytokine-induced T_H17 polarization. Gene silencing or chemical inhibition of p38/MAPK, NFAT5 or SGK1 abrogates the high-salt-induced T_H17 cell development. The T_H17 cells generated under high-salt conditions display a highly pathogenic and stable phenotype characterized by the upregulation of the pro-inflammatory cytokines GM-CSF, TNF-α and IL-2. Moreover, mice fed with a high-salt diet develop a more severe form of EAE, in line with augmented central nervous system infiltrating and peripherally induced antigen-specific T_H17 cells. Thus, increased dietary salt intake might represent an environmental risk factor for the development of autoimmune diseases through the induction of pathogenic T_H17 cells.

Although we have recently elucidated many of the genetic variants underlying the risk of developing autoimmune diseases[1], the significant increase in disease incidence, particularly of multiple sclerosis and type 1 diabetes, indicates that there have been fundamental changes in the environment that cannot be related to genetic factors. Diet has long been postulated as a potential environmental risk factor for this increasing incidence of autoimmune diseases in developed countries over recent decades[3]. One such dietary factor, which rapidly changed along with the Western diet and increased consumption of processed foods or 'fast foods', is salt (NaCl)[4,5]. The salt content in processed foods can be more than 100 times higher in comparison to similar home-made meals[5,6].

We have shown that excess NaCl uptake can affect the innate immune system[7]. Macrophages residing in the skin interstitium modulate local electrolyte composition in response to NaCl-mediated extracellular hypertonicity, and their regulatory activity provides a buffering mechanism for salt-sensitive hypertension[7]. Moreover, blockade of the renin-angiotensin system, can modulate immune responses and affect EAE[8,9]. Thus, to investigate whether increased NaCl intake might have a direct effect on $CD4^+$ T-cell populations and therefore represents a risk factor for autoimmune diseases, we investigated the effect of NaCl on the *in vitro* differentiation of human T_H17 cells. We induced hypertonicity by increasing NaCl concentration by 10–40 mM (high-salt) in the culture medium and thus mimicked concentrations that could be found in the interstitium of animals fed a high-salt diet[7]. As we previously reported, T_H17-promoting conditions for naive $CD4^+$ cells only induced a mild T_H17 phenotype[10]. Surprisingly, stimulation under increased NaCl concentrations markedly induced naive $CD4^+$ cell expression of IL-17A as determined by flow cytometry

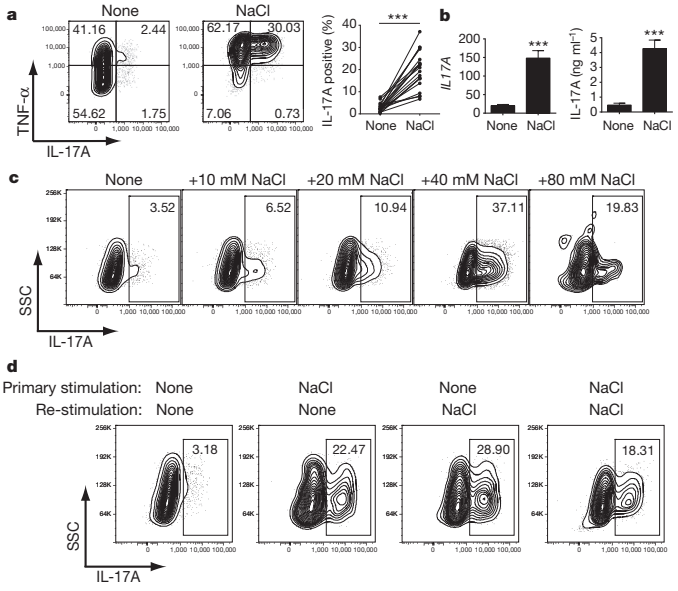

Figure 1 | Sodium chloride promotes the stable induction of T_H17 cells. **a**, Naive $CD4^+$ cells were differentiated into T_H17 cells in the presence (NaCl) or absence (none) of additional 40 mM NaCl and analysed by flow cytometry (FACS) for IL-17A ($n = 20$). **b**, IL-17A expression was measured by qRT–PCR (left panel, $n = 10$) and ELISA (right panel, $n = 5$). **c**, Cells were stimulated as in **a** under the indicated increased NaCl concentrations and analysed by FACS (one representative experiment of five is shown). **d**, Cells were stimulated as in **a** and were rested in the presence of IL-2. After 1 week, cells were re-stimulated as in **a** in the presence or absence of NaCl for another week and analysed by FACS (one representative experiment of five is shown). $***P < 0.001$. qRT–PCR data are depicted as relative expression. For all figures, error bars show, unless indicated elsewhere, mean ± s.e.m.

[1]Departments of Neurology and Immunobiology, Yale School of Medicine, 15 York Street, New Haven, Connecticut 06520, USA. [2]Broad Institute of MIT and Harvard, 7 Cambridge Center, Cambridge, Massachusetts 02142, USA. [3]Department of Neurology, University of Erlangen-Nuremberg, Schwabachanlage 6, 91054 Erlangen, Germany. [4]International Graduate School of Neuroscience, Ruhr-University Bochum, Universitätsstr. 150, 44801 Bochum, Germany. [5]Division of Clinical Pharmacology, Vanderbilt University, 2213 Garland Avenue, Nashville, Tennessee 37232, USA. [6]Interdisciplinary Center for Clinical Research and Department for Nephrology and Hypertension, University of Erlangen-Nuremberg, Glückstr. 6, 91054 Erlangen, Germany. [7]Experimental and Clinical Research Center, a joint cooperation between the Charité Medical Faculty and the Max-Delbrück Center for Molecular Medicine, Lindenberger Weg 80, 13125 Berlin, Germany. [8]Helios Klinikum Berlin-Buch, Schwanebecker Chaussee 50, 13125 Berlin, Germany. [9]Nikolaus-Fiebiger-Center for Molecular Medicine, University of Erlangen-Nuremberg, Glückstr. 6, 91054 Erlangen, Germany.
*These authors contributed equally to this work.

(Fig. 1a) or by quantitative polymerase chain reaction with reverse transcription (qRT–PCR) and enzyme-linked immunosorbent assay (ELISA) (Fig. 1b). The effect was dose dependent and an optimum of IL-17A induction was achieved by adding 40 mM NaCl in the presence of T_H17-inducing cytokines (TGF-β1, IL-1β, IL-6, IL-21, IL-23) (Fig. 1c and Supplementary Fig. 1). As expected, TNF-α was also induced[11], and increasing salt concentrations further led to cell death (data not shown). Nevertheless, adding 40 mM NaCl was tolerated by $CD4^+$ cells with little effect on growth or apoptosis (Supplementary Fig. 2). We then examined whether the nature of cation, anion, or osmolarity drives the increases in IL-17A secretion. We found that adding 40 mM sodium gluconate delivered an almost similar degree of T_H17 induction, whereas mannitol or $MgCl_2$ had only a slight effect. Moreover, 80 mM urea, an osmolyte able to pass through cell membranes, had no effect (Supplementary Fig. 3). Thus, the sodium cation was critical for IL-17A induction. We next examined the stability of the salt-induced effect. Naive $CD4^+$ cells that were initially stimulated under high-salt conditions continued to express increased amounts of IL-17A if re-stimulated under normal-salt conditions but could not be further induced with additional salt re-stimulation (Fig. 1d). This is consistent with the observation that only naive but not memory $CD4^+$ cells respond efficiently to increased salt concentrations (Supplementary Fig. 4). The high-salt effect was also observed when T_H17 cells were induced by antigen-specific stimulation (Supplementary Fig. 5)[12]. Furthermore, the effect was largely specific for T_H17 cells, as we did not observe comparable outcomes on differentiation of T_H1 or T_H2 cells (Supplementary Fig. 6).

To examine the mechanisms of enhanced IL-17A induction we performed a microarray analysis of naive $CD4^+$ T cells differentiated in the presence or absence of high-salt conditions (Fig. 2a and Supplementary Fig. 8). These data confirmed that cells displayed a stronger T_H17 phenotype under high-salt conditions, as most key signatures of T_H17 cells[2,13] including *CCL20*, *IL17F*, *RORC* and *IL23R* expression were highly upregulated. The analysis of the microarray data and its verification on messenger RNA or protein expression indicated that high-salt conditions induce a pathogenic type of T_H17 cells[14]. In addition to IL-17A, high NaCl concentration induced the expression of pro-inflammatory cytokines IL-2, TNF-α, IL-9 and several chemokines. These cells also upregulated CSF2 (also called GM-CSF), which is essential for the pathogenicity of T_H17 cells[15,16], and CCR6, which is crucial for T_H17 function in autoimmune disease[17]. Furthermore, *MIR155HG* (also called *MIRHG2*), the host gene for the microRNA miR-155 which is necessary for T_H17-induced EAE, was highly upregulated[18]. The high-salt-induced T_H17 cells also expressed more TBX21 (also called T-bet) and less GATA3 and *CXCR6* (Fig. 2a, b and Supplementary Figs 7 and 8, and data not shown). In total, these observations indicate that increased NaCl concentrations specifically promote the generation of a highly pathogenic T_H17 cell type[14].

We then examined the pathways whereby high-salt concentration induced this inflammatory phenotype. It has been shown that increased NaCl concentrations associated with augmented hypertonicity could induce immune system activation[11,19]. Moreover, it is known that hypertonic stress in mammals is sensed through p38/MAPK, a homologue to HOG1, the ancient yeast hypertonic stress-response element[19]. The key translator of this cascade is the osmosensitive transcription factor NFAT5 (refs 20, 21). Analysis of the microarray data set indicated the stimulation of both inflammatory and classic hypertonicity induced pathways. The $CD4^+$ cells expressed high levels of the NFAT5 targets *SGK1* (ref. 22) and the sodium/myo-inositol co-transporter *SLC5A3* (Fig. 2a, b and Supplementary Figs 7 and 8)[21,23]. Therefore, we proposed that increased NaCl concentration leads to phosphorylation of p38/MAPK that activates other downstream targets, including NFAT5. The phosphorylation of p38/MAPK was indeed increased in the presence of high-salt conditions (Fig. 3a and Supplementary Fig. 9a) and was accompanied by induction of *NFAT5* expression (Fig. 3c). We then determined whether inhibition of the p38/MAPK pathway influenced the effect. SB202190, an inhibitor of p38/MAPK[21] (p38i), only partially decreased *NFAT5* mRNA induction (Fig. 3c); however, SB202190 sharply reduced T_H17 polarization (Fig. 3b). In line with these findings, short interfering RNA (siRNA)-mediated knockdown of *MAPK14* in $CD4^+$ cells led to less IL-17A production (Supplementary Fig. 9b). High-salt concentration could also promote p38/MAPK activation via the release of ATP[24]. However, by interfering with this pathway we could not observe significant changes on T_H17 differentiation (data not shown).

Our data indicate that NFAT5 is involved in this NaCl-induced inflammatory pathway. Because it has been shown previously that NFAT5 influences responses of immune cells under similar conditions[7,20,21], we silenced *NFAT5* by a short hairpin RNA (shRNA) in naive $CD4^+$ cells. As expected, *NFAT5* silencing reduced *SLC5A3* expression, but also decreased IL-17A and CCR6 expression (Fig. 3d). A direct downstream target of NFAT5 is *SGK1* (ref. 22). Besides being activated by tonicity-dependent signals[25,26], *SGK1* expression is also regulated by TGF-β[27] and glucocorticoids[28]. As *SGK1* activation can be regulated by p38/MAPK[26,29] and NFAT5[22], and was strongly upregulated in the microarray, it was of interest to examine whether this kinase has a role in high-salt-mediated T_H17 polarization. *SGK1* was upregulated in naive $CD4^+$ cells after stimulation with high-salt conditions. To confirm that *SGK1* is regulated by p38/MAPK-dependent signals, expression of *SGK1* was measured in the presence of SB202190 (Fig. 3e). The addition of p38i reduced NaCl-induced *SGK1* mRNA expression, consistent with previous reports in other systems[22,26,29]. Moreover, shRNA-mediated silencing of *SGK1* significantly decreased IL-17A production in high-salt exposed cells and led to diminished CCR6 expression (Fig. 3f). In line with these observations, pharmacological blockade

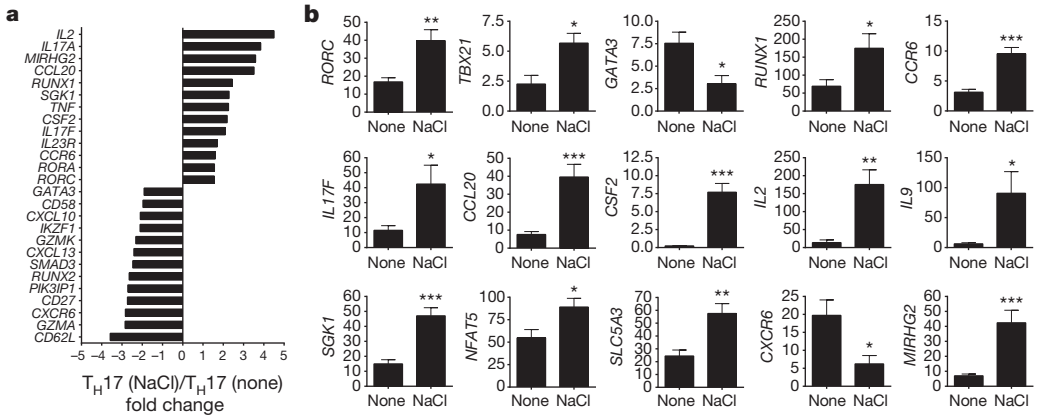

Figure 2 | High-salt-induced T_H17 cells display a pathogenic phenotype. **a**, Microarray analysis of naive $CD4^+$ cells differentiated into T_H17 cells in the presence (NaCl) or absence (none) of additional 40 mM NaCl. Depicted is a selection of 26 up- and downregulated genes (mean fold change of two independent experiments). **b**, qRT–PCR analysis of differentially expressed genes in the two groups ($n = 5$–8). $^*P < 0.05$, $^{**}P < 0.01$, $^{***}P < 0.001$.

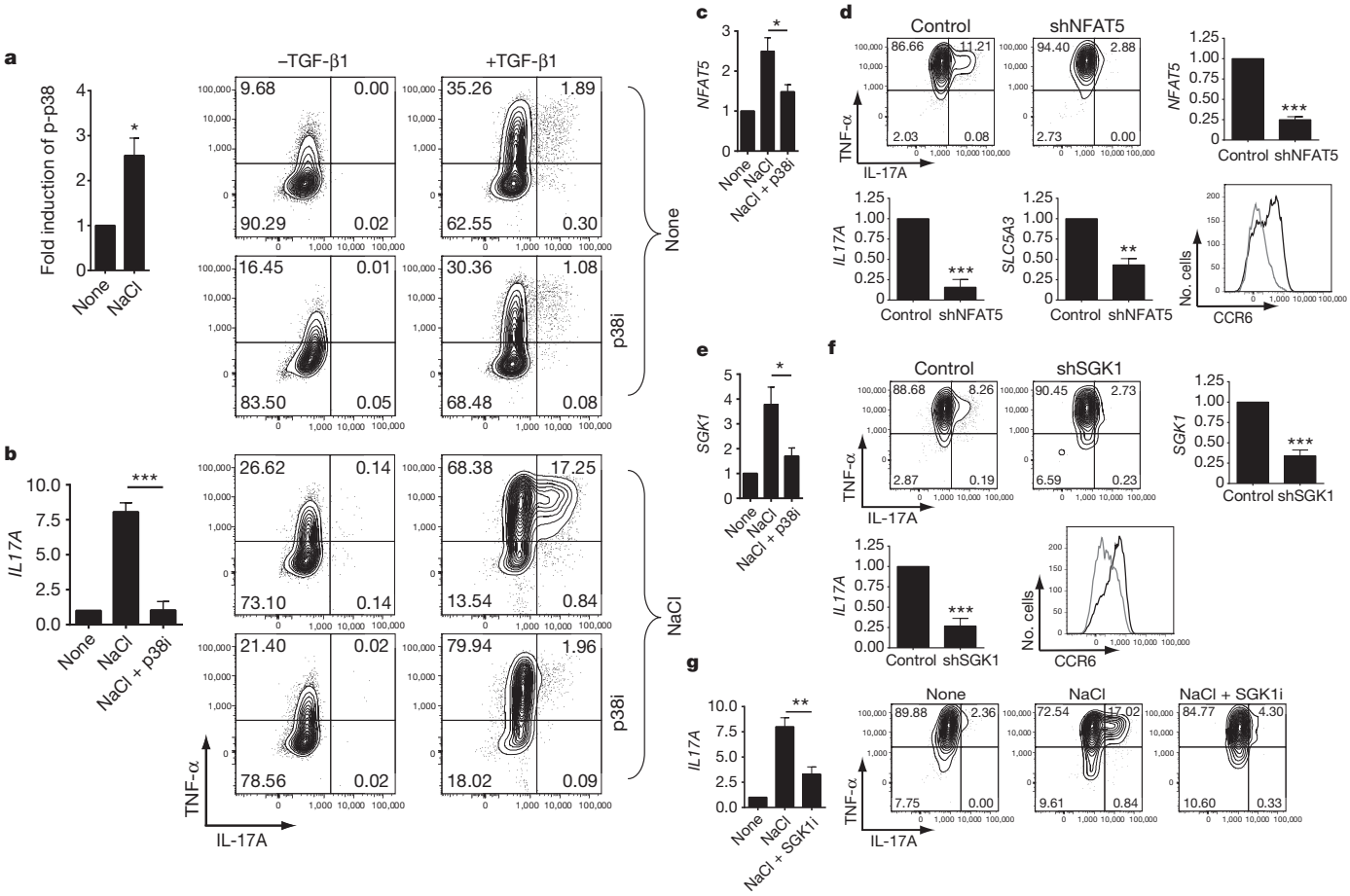

Figure 3 | The induction of T_H17 cells by NaCl depends on p38/MAPK, NFAT5 and SGK1. **a**, Naive $CD4^+$ cells were stimulated in the presence (NaCl) or absence (none) of additional 40 mM NaCl and were analysed by FACS for phosphorylated p38 (p-p38; $n = 5$). **b**, Naive $CD4^+$ cells were differentiated into T_H17 cells as indicated in the presence or absence of NaCl and SB202190 (p38i) and analysed by qRT–PCR as depicted in the bar graph ($n = 7$) or by FACS (the left row shows cells differentiated in the absence of TGF-β1). **c**, Naive $CD4^+$ cells were stimulated for 3 h in the presence or absence of NaCl and SB202190 and analysed by qRT–PCR for *NFAT5* ($n = 4$). **d**, Cells were transduced with NFAT5-specific (shNFAT5) or control shRNA (control), stimulated as in **b** and analysed by FACS. The bar graphs depict qRT–PCR analyses of *NFAT5*, *IL17A* and *SLC5A3* ($n = 5$). CCR6 was analysed by FACS (black histogram, control; grey histogram, shNFAT5; displayed as cell number versus CCR6; one representative experiment of four is shown). **e**, Cells were stimulated as in **c** but analysed by qRT–PCR for *SGK1* ($n = 4$). **f**, Cells were transduced with a shRNA specific for *SGK1* (shSGK1) or a control shRNA (control) and activated as in **b**, and analysed by FACS. Expression of *SGK1* and *IL17A* was determined by qRT–PCR ($n = 5$). CCR6 was analysed by FACS (black histogram, control; grey histogram, shSGK1; displayed as cell number versus CCR6; one representative experiment of four is shown). **g**, Cells were cultured as in **b** but in the presence or absence of the SGK1 inhibitor GSK650394 (SGK1i) and analysed by FACS. The bar graph shows qRT–PCR for *IL17A* under similar conditions ($n = 5$). FACS and qRT–PCR (relative expression) data depicted in bar graphs were normalized to controls. $*P < 0.05$, $**P < 0.01$, $***P < 0.001$.

of SGK1 produced similar, albeit less pronounced, results compared to SB202190 (Fig. 3g).

The rather dramatic *in vitro* effects of high-salt concentration on naive human $CD4^+$ cells prompted us to examine the effects of increased dietary NaCl in an *in vivo* system. We first adapted the human culture system to various murine T_H17 differentiation models and made similar observations of increased T_H17 induction and the accompanying phenotype (Fig. 4 and Supplementary Fig. 10). High-salt conditions did not significantly alter proliferation or cell death. Moreover, the effect was specific for T_H17 conditions, as there was no enhancement of T_H1 or T_H2 differentiations (Supplementary Figs 11 and 12 and data not shown). High-salt-induced expression of *Nfat5*, *Sgk1* and IL-17A was dependent on p38/MAPK. Enhanced T_H17 differentiation could be blocked by SB202190, and gene deletion of p38α decreased *Il17a*, *Nfat5* and *Sgk1* induction (Supplementary Figs 10 and 13). As the high-salt effect on T_H17 cells appeared similar between species, we examined whether dietary NaCl influenced EAE. High-salt diet accelerated onset and increased severity of the disease (Fig. 4c), whereas blood pressure was not affected (Supplementary Fig. 14). Mice on the high-salt diet displayed significantly higher numbers of CNS-infiltrating $CD3^+$ and $Mac3^+$ cells compared to controls (Fig. 4c). IL-17A-expressing $CD4^+$ cells in CNS infiltrates almost doubled in frequency and, accordingly, we detected increased *Il17a* and *Rorc* mRNA expression in spinal cords (Fig. 4d and Supplementary Fig. 15). In contrast to *Ifng*, we found augmented expression of *Il17a* and *Csf2* and higher levels of *Nfat5* and *Sgk1* in the spleens of high-salt diet EAE mice compared to controls (Fig. 4e). Notably, splenocytes from EAE mice fed the high-salt diet showed enhanced IL-17A but not IFN-γ or T_H2 cytokine expression upon antigen re-stimulation, indicating increased *in vivo* induction of antigen-specific T_H17 cells (Fig. 4f and data not shown). Consistent with *in vitro* data, the high-salt-diet-induced effect was dependent on p38/MAPK, as *in vivo* administration of SB202190 inhibited salt-induced increases in the frequency of T_H17 cells infiltrating the CNS (Supplementary Fig. 15b, c).

In this investigation, we found that modest increases in NaCl concentration could stimulate an almost logarithmic *in vitro* induction of IL-17A in naive $CD4^+$ cells mediated through p38/MAPK, NFAT5 and SGK1. Importantly, the addition of 40 mM of NaCl to T_H17 differentiation cultures not only increased IL-17A expression but also led to a pathogenic phenotype of T_H17 cells. In line with these findings, common salt added to the diet of mice led to severe worsening of EAE accompanied by increased numbers of T_H17 cells.

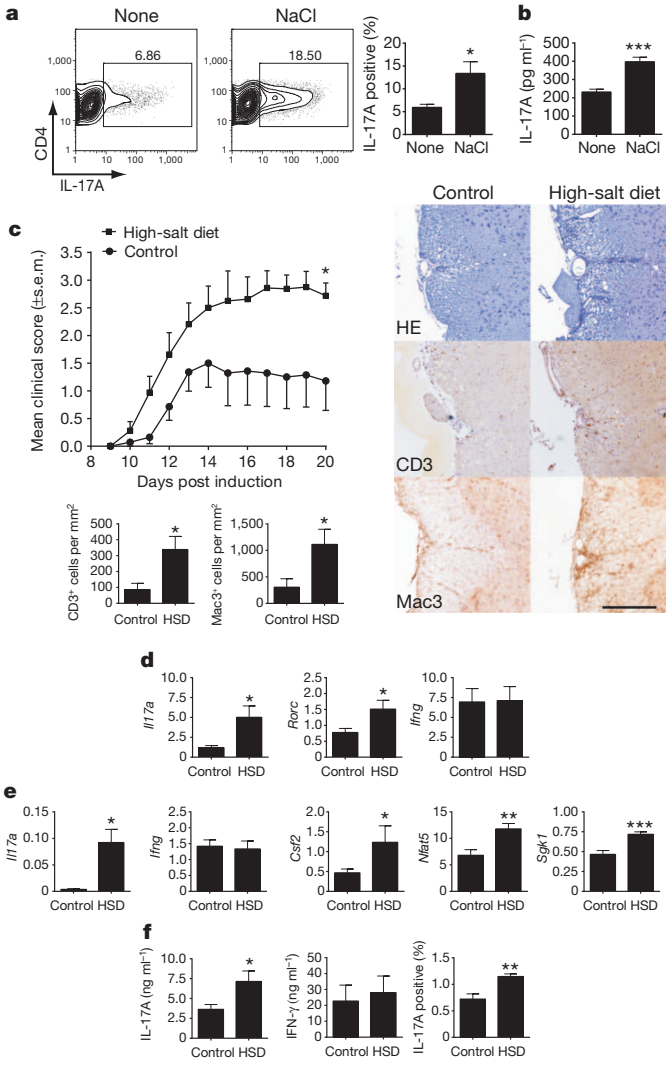

Figure 4 | High-salt diet induces T_H17 cells *in vivo* and exacerbates experimental autoimmune encephalomyelitis. **a**, Naive murine $CD4^+$ cells were stimulated with radiated APCs, anti-CD3, IL-6 and TGF-β1 in the presence (NaCl) or absence (none) of additional 40 mM NaCl and were analysed by FACS ($n = 3$). **b**, IL-17A secretion (ELISA) of primary splenocytes, stimulated by anti-CD3 in the presence or absence of NaCl ($n = 6$). **c**, Mean clinical scores of EAE in high-salt diet (HSD) animals (squares) or controls (dots, pooled data of two independent experiments with 12 animals). Histological analyses (right) show sections of the spinal cord stained with haematoxylin and eosin (HE), anti-CD3 and anti-Mac3 for control or HSD animals (scale bar, 100 μM) and were quantified for CD3 and Mac3 (bar graphs, $n = 5$–6). **d**, Spinal cord from EAE animals was analysed by qRT–PCR ($n = 5$–6). **e**, Splenocytes from EAE animals were analysed by qRT–PCR ($n = 4$–7). **f**, Splenocytes from EAE animals were re-stimulated with MOG for 2 days and supernatants were analysed for IL-17A and IFN-γ by ELISA ($n = 7$–8) or cells were analysed for IL-17A by FACS ($n = 4$). qRT–PCR data are depicted as relative expression. $^*P < 0.05$; $^{**}P < 0.01$; $^{***}P < 0.001$.

What might be the physiological role for the effect of high-salt on the induction of inflammatory T_H17 cells? The concentration of Na^+ in plasma is approximately 140 mM, similar to standard cell culture media. Less well appreciated is that in the interstitium and lymphoid tissue, considerably higher Na^+ concentrations between 160 mM and even as high as 250 mM can be encountered[7,20]—the 'high-salt' conditions that we found to induce inflammatory T_H17 cells. Thus, this may be a mechanism for decreasing immune activation in the blood while favouring an inflammatory response in lymphoid tissues or with migration of cells into tissue. In this context it could be expected that other immune cells can react on high-salt conditions as well and potentially contribute to the effects observed *in vivo*.

Do these data indicate that increased salt intake is the long-sought-after environmental factor associated with the epidemic of autoimmune disease? Although these data present an attractive hypothesis, the direct causality of salt intake and incidence of autoimmune disease is yet to be demonstrated. That is, no *in vitro* observation can prove causality in humans; instead, our data indicate that clinical trials with severe curtailment of salt intake for individuals at risk for developing autoimmune disease are required. Clinical scenarios in which a dietary salt restriction protocol could be tested are multiple sclerosis or psoriasis, both autoimmune diseases with strong T_H17 components[2]. Additionally, excess salt content in diet should be investigated as a potential environmental risk factor for autoimmune diseases. However, this study would be difficult in Western cultures where the application of a true low-salt diet, representing the conditions in which *Homo sapiens* were environmentally selected in Africa, is difficult to achieve. Nevertheless, although there might be additional mechanisms contributing to the observed effects, the pathways identified in this study may offer new targets for the treatment of autoimmune diseases, with interference in the p38/MAPK, NFAT5 and SGK1 pathways aimed at blocking the generation of pathogenic T_H17 cells.

METHODS SUMMARY

Human cell sorting. Peripheral blood mononuclear cells (PBMCs) were obtained from the peripheral blood of healthy subjects in compliance with institutional review board (IRB) protocols. $CD4^+$ T cells were isolated by negative selection using magnetic beads (Miltenyi Biotec). Subsequently, naive T cell were sorted as $CD4^+CD25^-CD127^+CD45RO^-CD45RA^+$ and memory cells were obtained by sorting for $CD4^+CD25^-CD127^+CD45RO^+CD45RA^-$ on a FACS Aria (BD Biosciences).

Human differentiation assays. Naive, memory or total $CD4^+$ T cells were stimulated by plate-bound anti-CD3 and soluble anti-CD28 in serum-free X-VIVO15 medium (BioWhittaker) where indicated in the presence of various cytokines (IL-1β, IL-6, IL-21, IL-23, TGF-β1) and different concentrations of NaCl. Cells were analysed for cytokine expression by intracellular flow cytometry. Cytokine secretion was measured by ELISA (eBioscience). mRNA expression was determined by quantitative RT–PCR (Applied Biosystems).

EAE induction and high-salt diet. Male C57BL/6J mice (Harlan) were immunized with 200 μg MOG_{35-55} in an equal amount of complete Freund's adjuvant and received 200 ng pertussis toxin intraperitoneally on days 0 and 2 post induction. The clinical evaluation was performed daily on a 5 point scale ranging from 0 (no clinical sign) to 5 (moribund). Mice received normal chow and tap water ad libitum (control) or sodium-rich chow containing 4% NaCl and tap water containing 1% NaCl ad libitum (high-salt diet).

Full Methods and any associated references are available in the online version of the paper.

Received 13 March; accepted 19 December 2012.
Published online 6 March 2013.

1. International Multiple Sclerosis Genetics Consortium & Wellcome Trust Case Control Consortium. Genetic risk and a primary role for cell-mediated immune mechanisms in multiple sclerosis. *Nature* **476,** 214–219 (2011).
2. Korn, T., Bettelli, E., Oukka, M. & Kuchroo, V. K. IL-17 and Th17 Cells. *Annu. Rev. Immunol.* **27,** 485–517 (2009).
3. Ascherio, A. & Munger, K. L. Environmental risk factors for multiple sclerosis. Part II: Noninfectious factors. *Ann. Neurol.* **61,** 504–513 (2007).
4. McGuire, S. Institute of Medicine. 2010. Strategies to reduce sodium intake in the United States. Washington, DC: The National Academies Press. *Adv. Nutr.* **1,** 49–50 (2010).
5. Appel, L. J. *et al.* The importance of population-wide sodium reduction as a means to prevent cardiovascular disease and stroke: a call to action from the American Heart Association. *Circulation* **123,** 1138–1143 (2011).
6. Brown, I. J., Tzoulaki, I., Candeias, V. & Elliott, P. Salt intakes around the world: implications for public health. *Int. J. Epidemiol.* **38,** 791–813 (2009).
7. Machnik, A. *et al.* Macrophages regulate salt-dependent volume and blood pressure by a vascular endothelial growth factor-C-dependent buffering mechanism. *Nature Med.* **15,** 545–552 (2009).
8. Platten, M. *et al.* Blocking angiotensin-converting enzyme induces potent regulatory T cells and modulates TH1- and TH17-mediated autoimmunity. *Proc. Natl Acad. Sci. USA* **106,** 14948–14953 (2009).
9. Stegbauer, J. *et al.* Role of the renin-angiotensin system in autoimmune inflammation of the central nervous system. *Proc. Natl Acad. Sci. USA* **106,** 14942–14947 (2009).

10. Yang, L. *et al.* IL-21 and TGF-β are required for differentiation of human T_H17 cells. *Nature* **454,** 350–352 (2008).
11. Junger, W. G., Liu, F. C., Loomis, W. H. & Hoyt, D. B. Hypertonic saline enhances cellular immune function. *Circ. Shock* **42,** 190–196 (1994).
12. Zielinski, C. E. *et al.* Pathogen-induced human TH17 cells produce IFN-γ or IL-10 and are regulated by IL-1β. *Nature* **484,** 514–518 (2012).
13. Zhou, L. & Littman, D. R. Transcriptional regulatory networks in Th17 cell differentiation. *Curr. Opin. Immunol.* **21,** 146–152 (2009).
14. Ghoreschi, K. *et al.* Generation of pathogenic T_H17 cells in the absence of TGF-β signalling. *Nature* **467,** 967–971 (2010).
15. Codarri, L. *et al.* RORγt drives production of the cytokine GM-CSF in helper T cells, which is essential for the effector phase of autoimmune neuroinflammation. *Nature Immunol.* **12,** 560–567 (2011).
16. El-Behi, M. *et al.* The encephalitogenicity of T_H17 cells is dependent on IL-1- and IL-23-induced production of the cytokine GM-CSF. *Nature Immunol.* **12,** 568–575 (2011).
17. Reboldi, A. *et al.* C–C chemokine receptor 6-regulated entry of T_H-17 cells into the CNS through the choroid plexus is required for the initiation of EAE. *Nature Immunol.* **10,** 514–523 (2009).
18. O'Connell, R. M. *et al.* MicroRNA-155 promotes autoimmune inflammation by enhancing inflammatory T cell development. *Immunity* **33,** 607–619 (2010).
19. Shapiro, L. & Dinarello, C. A. Osmotic regulation of cytokine synthesis *in vitro*. *Proc. Natl Acad. Sci. USA* **92,** 12230–12234 (1995).
20. Go, W. Y., Liu, X., Roti, M. A., Liu, F. & Ho, S. N. NFAT5/TonEBP mutant mice define osmotic stress as a critical feature of the lymphoid microenvironment. *Proc. Natl Acad. Sci. USA* **101,** 10673–10678 (2004).
21. Kino, T. *et al.* Brx mediates the response of lymphocytes to osmotic stress through the activation of NFAT5. *Sci. Signal.* **2,** ra5 (2009).
22. Chen, S. *et al.* Tonicity-dependent induction of Sgk1 expression has a potential role in dehydration-induced natriuresis in rodents. *J. Clin. Invest.* **119,** 1647–1658 (2009).
23. Ortells, M. C. *et al.* Transcriptional regulation of gene expression during osmotic stress responses by the mammalian target of rapamycin. *Nucleic Acids Res.* **40,** 4368–4384 (2012).
24. Woehrle, T. *et al.* Hypertonic stress regulates T cell function via pannexin-1 hemichannels and P2X receptors. *J. Leukoc. Biol.* **88,** 1181–1189 (2010).
25. Waldegger, S., Barth, P., Raber, G. & Lang, F. Cloning and characterization of a putative human serine/threonine protein kinase transcriptionally modified during anisotonic and isotonic alterations of cell volume. *Proc. Natl Acad. Sci. USA* **94,** 4440–4445 (1997).
26. Bell, L. M. *et al.* Hyperosmotic stress stimulates promoter activity and regulates cellular utilization of the serum- and glucocorticoid-inducible protein kinase (Sgk) by a p38 MAPK-dependent pathway. *J. Biol. Chem.* **275,** 25262–25272 (2000).
27. Waldegger, S. *et al. h-sgk* serine-threonine protein kinase gene as transcriptional target of transforming growth factor β in human intestine. *Gastroenterology* **116,** 1081–1088 (1999).
28. Webster, M. K., Goya, L., Ge, Y., Maiyar, A. C. & Firestone, G. L. Characterization of sgk, a novel member of the serine/threonine protein kinase gene family which is transcriptionally induced by glucocorticoids and serum. *Mol. Cell. Biol.* **13,** 2031–2040 (1993).
29. Waldegger, S., Gabrysch, S., Barth, P., Fillon, S. & Lang, F. h-sgk serine-threonine protein kinase as transcriptional target of p38/MAP kinase pathway in HepG2 human hepatoma cells. *Cell. Physiol. Biochem.* **10,** 203–208 (2000).

Supplementary Information is available in the online version of the paper.

Acknowledgements The authors would like to thank S. Bhela, M. Zaidi, P. Quass, M. Mroz and S. Seubert for technical assistance and F. C. Luft for critical reading of the manuscript. We are grateful to J.-P. David and S. Teufel for providing Mx-Cre^+ $p38\alpha^{fl/fl}$ mice. This work was supported by a National MS Society Collaborative Research Center Award CA1061-A-18, National Institutes of Health Grants P01 AI045757, U19 AI046130, U19 AI070352, and P01 AI039671, and by a Jacob Javits Merit award (NS2427) from the National Institute of Neurological Disorders and Stroke, the Penates Foundation and the Nancy Taylor Foundation for Chronic Diseases, Inc. (to D.A.H.). R.A.L. was supported by the ELAN programme, University of Erlangen. D.N.M. was supported by the German Research Foundation (DFG) and the German Center for Cardiovascular Research (DZHK). J.T. was supported by the Interdisciplinary Center for Clinical Research at University of Erlangen and the German Research Foundation.

Author Contributions M.K. designed the study, planned and performed experiments, analysed data and wrote the manuscript. A.M. planned and performed experiments, analysed data and wrote the manuscript. J.T. and H.K. interpreted data and supported the work with key suggestions and editing the manuscript. N.Y. analysed data. R.A.L. planned experiments, analysed data and wrote the manuscript. D.N.M. designed the study, planned experiments, analysed data and wrote the manuscript. D.A.H. designed the study, planned experiments, analysed data, and wrote the manuscript. M.K., D.N.M. and D.A.H. co-directed the project.

Author Information The microarray data sets have been deposited in the Gene Expression Omnibus database under accession number GSE42569. Reprints and permissions information is available at www.nature.com/reprints. The authors declare no competing financial interests. Readers are welcome to comment on the online version of the paper. Correspondence and requests for materials should be addressed to M.K. (markus.kleinewietfeld@yale.edu) or D.A.H. (david.hafler@yale.edu).

METHODS

Antibodies, recombinant cytokines and reagents. The following monoclonal antibodies and reagents were used as follows: for surface staining, anti-CD4 (RPA-T4), anti-CD45RO (UCHL1), anti-CD45RA (HI100), anti-CD25 (M-A251), anti-CD127 (hIL-7R-M21), anti-CCR6 (11A9) and AnnexinV all from BD Biosciences; for intracellular staining, anti-IL-17A (eBio64DEC17), anti-TNF-α (MAb11), anti-IFN-γ (4S.B3), anti-IL-2 (MQ1-17H12), anti-RORC (AFKJS-9), anti-GATA3 (TWAJ) and anti-Tbet (eBio4B10) from eBioscience, and anti-pp38 (36/p38) (BD Biosciences) and anti-GM-CSF (BVD2-21C11) from Biolegend; for T-cell stimulation, anti-CD3 (UCHT1) and anti-CD28 (28.2) from BD Biosciences. Recombinant human TGF-β1 was purchased from eBioscience, recombinant human IL-1β, IL-6, IL-4, IL-12 and IL-23 and neutralizing anti-IFN-γ (25718) and anti-IL-4 (3007) were purchased from R&D Systems, and recombinant human IL-21 was purchased from Cell Sciences. CFSE was obtained from Invitrogen.

Human cell isolation and stimulation. Peripheral blood was obtained from healthy control volunteers in compliance with Institutional Review Board protocols. Peripheral blood mononuclear cells (PBMCs) were separated by Ficoll-Paque PLUS (GE Healthcare) gradient centrifugation. Untouched total $CD4^+$ T cells were isolated from PBMCs by negative selection via the $CD4^+$ T-cell isolation kit II (Miltenyi Biotec). Naive ($CD45RA^+CD45RO^-CD25^-CD127^+$) and memory ($CD45RA^-CD45RO^+CD25^-CD127^+$) $CD4^+$ T cells were sorted by high-speed flow cytometry with a FACS Aria (BD Biosciences) to a purity >98% as verified by post-sort analysis. Dead cells were excluded by propidium iodide (BD Biosciences). $CD14^+$ monocytes were isolated by positive selection with CD14 microbeads (Miltenyi Biotec). Cells were cultured in 96-well round-bottom plates (Costar) at 5×10^4 cells per well in serum-free X-VIVO15 medium (BioWhittaker), and stimulated with plate-bound anti-CD3 (10 μg ml^{-1}) and soluble anti-CD28 (1 μg ml^{-1}) antibodies. Where indicated, recombinant TGF-β1 (5 ng ml^{-1}), IL-1β (12.5 ng ml^{-1}), IL-6 (25 ng ml^{-1}), IL-21 (25 ng ml^{-1}), or IL-23 (25 ng ml^{-1}) or additional 10–80 mM NaCl was added to the cultures. For T_H1 and T_H2 differentiation, naive cells were stimulated as described above but in the presence of IL-12 (10 ng ml^{-1}) and anti-IL-4 (10 μg ml^{-1}) (for T_H1 cells) or with IL-4 (10 ng ml^{-1}) and anti-IFN-γ (10 μg ml^{-1}) (for T_H2 cells). In some experiments the specific inhibitors SB202190 (Sigma Aldrich) or GSK650394[30] (Tocris Bioscience/R&D Systems) at concentrations of 5 μM or 1 μM, respectively, were added to the cultures. Co-cultures of $CD14^+$ monocytes and T cells were performed as described before[12]. In brief, monocytes were pulsed for 3 h with *Candida albicans* (GREER) and irradiated (45 Gy) before T cell co-culture (ratio of 1:2). Total $CD4^+$ T cells were co-cultured for 12 days and naive $CD4^+$ T cells were co-cultured for 7 days in the presence of additional cytokine cocktail (TGF-β1, IL-1β, IL-6, IL-21 and IL-23). Recombinant human IL-2 was obtained through the AIDS Research and Reference Reagent Program, Division of AIDS, National Institute of Allergy and Infectious Diseases (NIAID), National Institutes of Health (NIH) and was used for re-stimulation experiments at 20 U ml^{-1}. Cells were cultured for the indicated periods of time.

Flow cytometry and cytokine detection. Cells were analysed by flow cytometry if not specified elsewhere after a culture period between 7 and 8 days. For surface staining, cells were stained with the respective antibodies for 20 min in PBS containing 0.5% FCS and 2 mM EDTA before analysis. For intracellular staining, cells were stimulated for 4–5 h with PMA (50 ng ml^{-1}) and ionomycin (250 ng ml^{-1}; both from Sigma-Aldrich) in the presence of GolgiPlug (BD Biosciences), fixed and made permeable (Fix/Perm; eBioscience) according to the manufacturer's instructions, and stained with the respective antibodies for intracellular cytokine detection for 30–45 min. Before fixation, cells were stained with the LIVE/DEAD cell kit (Invitrogen) to exclude dead cells. For measurement of phosphorylated p38 (p-p38), cells were stimulated for 20 min before cells were fixed (Cytofix buffer, BD Biosciences) and made permeable (Phosflow Perm Buffer III, BD Biosciences) according to the manufacturer's instructions and stained for 30–45 min with anti-p-p38. Data were acquired on a LSR II (BD Biosciences) and analysed with FlowJo software (TreeStar). Culture supernatants were taken on day 6 and measured by ELISA for secretion of IL-17A (eBioscience) according to the manufacturer's instructions.

Real-time PCR. Cells for RNA isolation were harvested if not specified elsewhere between 6 and 7 days of culture and RNA was isolated using the Absolutely RNA 96 Microprep kit (Agilent Technologies) or RNeasy micro kit (Qiagen) and converted to cDNA via reverse transcriptase by random hexamers and Multiscribe RT (TaqMan Gold RT–PCR kit, Applied Biosystems). All primers were purchased from Applied Biosystems. All reactions were performed on a StepOnePlus Real-Time PCR System (Applied Biosystems). The values are represented as the difference in Ct values normalized to β2-microglobulin for each sample as per the following formula: relative RNA expression = $(2^{-\Delta Ct}) \times 10^3$.

shRNA- and siRNA-mediated gene silencing. Lentiviral particles expressing shRNAs were obtained from the library of The RNAi Consortium (TRC)[31]. Lentiviral transduction of human T cells was carried out as described before[32]. In brief, 5×10^4 human naive $CD4^+$ T cells per well were stimulated for 24 h before infection. Cells were then transduced with viral particles containing a vector expressing the indicated specific shRNA or as controls a vector expressing an unspecific shRNA or expressing GFP. Transduction was mediated at a multiplicity of infection (MOI) of 5 by centrifugation at 2,250 r.p.m. for 30 min at room temperature in the presence of 3 μg ml^{-1} polybrene (Millipore). After 48 h puromycin (Invitrogen) was added to the cultures at a concentration of 0.5 μg ml^{-1} to select for successfully transduced cells and was controlled by flow cytometry for GFP and propidium iodide. The specific RNAi Consortium clones were TRCN0000020019 for NFAT5 and TRCN0000040175 for SGK1. For siRNA transfections, control siRNA (ON-TARGETplus non targeting 1) and a pool of four specific siRNAs for *MAPK14* (ON-TARGETplus SMARTpool 1432) were obtained from Thermo Scientific Dharmacon. Cells were transfected by using Human T Cell Nucleofector kit and a Nuclofector II device as recommended by the manufacturer (Lonza/Amaxa).

Microarray analysis. Cells for microarray analysis were collected at day 7 of culture and total RNA was isolated using Trizol reagent according to the manufacturer (Invitrogen). Expression data were generated by using GeneChip Human Genome U133 Plus 2.0 arrays (Affymetrix) at the Yale Center for Genome Analysis (YCGA). For analysis, the data were normalized using the GenePattern software[33] with the Robust Multi Array (RMA) algorithm[34]. The COMBAT software was used to remove batch effects. Fold change was computed between the average expression levels of each probe set in samples with the different conditions. To avoid spurious fold levels due to low expression values, a small constant ($c = 50$) was added to the expression values. Only cases where more than 50% of the four possible pair-wise comparisons were over a cutoff of 1.5-fold change were reported. A Z-score was computed as additional filter by comparing the mean of the expression levels in the NaCl-treated samples to the expression levels in the control samples. Only cases with a corresponding P-value lower than 0.05 were reported.

Western blotting. Western blotting was performed as described before[35]. Phospho-p38 was detected by using anti-phospho-p38 (Cell Signaling Technology). Anti-β-actin and anti-SGK1 antibodies were obtained from Cell Signaling Technology and anti-NFAT5 antibodies were purchased from Pierce/Thermo Scientific. Primary antibodies were detected by peroxidase-conjugated streptavidin (Jackson Immuno Research), secondary anti-rabbit-HRP-conjugated (Cell signalling Technology or Jackson Immuno Research) and secondary anti-mouse-HRP-conjugated (Bio-Rad) antibodies.

Mice, EAE induction, high-salt diet and blood pressure analysis. C57BL/6J mice were purchased from Harlan and housed at the in-house animal care facility of the University of Erlangen under standardized conditions. EAE induction was done as described before[9]. Briefly, male mice were immunized with 200 μg MOG_{35-55} (Charite) in an equal amount of complete Freund's adjuvant and received 200 ng pertussis toxin (List Biochemicals) intraperitoneally on days 0 and 2 post induction. The clinical evaluation was performed on a daily bases by a 5-point scale ranging from 0, no clinical sign; 1, limp tail; 2, limp tail, impaired righting reflex, and paresis of one limb; 3, hindlimb paralysis; 4, hindlimb and forelimb paralysis; 5, moribund. Mice received normal chow and tap water ad libitum (control group) or sodium-rich chow containing 4% NaCl (SSNIFF) and tap water containing 1% NaCl ad libitum (high-salt group). Inhibition of p38/MAPK *in vivo* was done as described before[36]. In brief, mice were maintained on a control or high-salt diet and either received 1 mg kg^{-1} d^{-1} SB202190 (TOCRIS) intraperitoneally or vehicle from day −3 post induction of EAE. Brain leukocytes were isolated by percoll gradient centrifugation on day 17 post EAE induction, stimulated by PMA/ionomycin and analysed by flow cytometry for IL-17A and CD4 expression. Mx-Cre^+/$p38\alpha^{fl/fl}$ mice[37] maintained on a C57BL/6 background were a gift from J.-P. David. Mice were injected with 13 mg kg^{-1} body weight polyinosinic-polycydidylic acid (poly(I:C), Sigma-Aldrich) on days 0, 2, 6 and were killed on day 8 for isolation of splenocytes. Blood pressure analysis was performed by the tail cuff method as described previously[9]. All animal experimentation was performed in accordance to the German animal protection law.

Histology. On day 20 post induction, mice were perfused with 4% paraformaldehyde and then the lumbar, thoracal and cervical part of their spinal cord was embedded in paraffin. Spinal cord cross-sections were stained with haematoxylin and eosin to assess inflammation. T cells were labelled by anti-CD3 (Serotec), macrophages/microglia by anti-Mac3 (BD Biosciences) and IL-17-positive cells by anti-IL-17 (Abcam).

Murine T-cell cultures. Splenic T cells from EAE animals were re-stimulated with 20 μg ml^{-1} MOG_{35-55} peptide for 48 h, for intracellular IL-17A detection, monensin (BD Biosciences) was added to the cultures for an additional 6 h. Splenic T cells from naive mice were stimulated with 1 μg ml^{-1} plate-bound anti-CD3 (17A2, BD Biosciences) and 1 μg ml^{-1} soluble anti-CD28 (37.51, BD

Biosciences) for 48 h. For T_H17 cell differentiation, spleen and lymph node cells from 10-week-old 2D2 mice[38] were pooled and $CD4^+CD62L^+$ naive T cells were isolated by magnetic cell sorting (Miltenyi Biotec). Cells were cultured at 2×10^6 cells ml^{-1} and stimulated for 4 days with 2×10^7 irradiated (30 Gy) syngenic splenocytes per ml and 1 μg ml^{-1} anti-CD3 (2C11, BD Biosciences) in the presence of TGF-β1 (5 ng ml^{-1}) and IL-6 (20 ng ml^{-1}) and where indicated of additional 40 mM NaCl. For APC free T_H17 differentiations, naive T cells were sorted as $CD4^+CD62L^+CD44^{lo}CD25^-$ and stimulated by plate-bound anti-CD3 (2 μg ml^{-1}) and anti-CD28 (2 μg ml^{-1}) in the presence of IL-6 (40 ng ml^{-1}) and TGF-β1 (1 ng ml^{-1}) or IL-6 (40 ng ml^{-1}) and IL-23 (10 ng ml^{-1}) (all from R&D Systems) and were cultured for 4 days. In some experiments, 10 μM SB202190 (TOCRIS) was added to the cultures. For T_H1 differentiation, naive $CD4^+$ T cells were cultured for 96 h with anti-CD3, anti-CD28, IL-12 (20 ng ml^{-1}) (BioLegend) and anti-IL-4 (10 μg ml^{-1}) (1B11, BioLegend). To monitor proliferation, cells were labelled with fixable proliferation dye (eBioscience) according to the manufacturer's protocol. For intracellular flow cytometry, cells were stimulated for 4 h with PMA/ionomycin in the presence of monensin and stained for CD4 (RM4-5, eBioscience) and intracellular IL-17A (eBio17B7, eBioscience), IFN-γ (XMG1.2, eBioscience), Tbet (4B10, eBioscience) or RORC/RORγt (AFKJS-9, eBioscience), excluding dead cells by a fixable viability dye (eBioscience). For murine gene expression analysis, mRNA was prepared using PeqLab Gold HP total RNA kit (PeqLab) and cDNA was prepared using superscript II reverse transcriptase (Invitrogen). RNA was isolated from EAE animals at day 14 post induction. Reactions were performed on a 7900 Sequence Detection System (Applied Biosystems). Primers were obtained from Applied Biosystems and target expression was normalized to β-actin expression. For cytokine secretion analysis, cells were stimulated as indicated and supernatants were collected after 3 days of culture. Monoclonal antibody pairs and recombinant cytokine standards were purchased from R&D systems (IL-17A, IFN-γ).

Statistical analysis. Statistical analysis was performed using GraphPad Prism (GraphPad Software). Data were analysed by an unpaired *t*-test in case of two groups and by one-way ANOVA using Tukey's post-hoc test in multiple groups. Data tested against a specified value were analysed by a one-sample *t*-test. EAE was analysed using a non-parametric Mann–Whitney *U*-test. Data were presented if not indicated elsewhere as mean ± s.e.m. $P < 0.05$ was considered to be statistically significant ($^*P < 0.05$, $^{**}P < 0.01$, $^{***}P < 0.001$).

30. Sherk, A. B. *et al.* Development of a small-molecule serum- and glucocorticoid-regulated kinase-1 antagonist and its evaluation as a prostate cancer therapeutic. *Cancer Res.* **68,** 7475–7483 (2008).
31. Moffat, J. *et al.* A lentiviral RNAi library for human and mouse genes applied to an arrayed viral high-content screen. *Cell* **124,** 1283–1298 (2006).
32. Astier, A. L. *et al.* RNA interference screen in primary human T cells reveals FLT3 as a modulator of IL-10 levels. *J. Immunol.* **184,** 685–693 (2010).
33. Reich, M. *et al.* GenePattern 2.0. *Nature Genet.* **38,** 500–501 (2006).
34. Irizarry, R. A. *et al.* Exploration, normalization, and summaries of high density oligonucleotide array probe level data. *Biostatistics* **4,** 249–264 (2003).
35. Wenzel, K. *et al.* Potential relevance of α1-adrenergic receptor autoantibodies in refractory hypertension. *PLoS ONE* **3,** e3742 (2008).
36. Noubade, R. *et al.* Activation of p38 MAPK in CD4 T cells controls IL-17 production and autoimmune encephalomyelitis. *Blood* **118,** 3290–3300 (2011).
37. Engel, F. B. *et al.* p38 MAP kinase inhibition enables proliferation of adult mammalian cardiomyocytes. *Genes Dev.* **19,** 1175–1187 (2005).
38. Bettelli, E. *et al.* Myelin oligodendrocyte glycoprotein-specific T cell receptor transgenic mice develop spontaneous autoimmune optic neuritis. *J. Exp. Med.* **197,** 1073–1081 (2003).